ARTICLE

Effective Extraction of Photoluminescence from a Diamond Layer with a Photonic Crystal

Lukáš Ondič,[†,‡,∥,*] Kateřina Dohnalová,[†,§] Martin Ledinský,[†] Alexander Kromka,[†] Oleg Babchenko,[†] and Bohuslav Rezek[†]

[†]Institute of Physics, Academy of Sciences of the Czech Republic, v.v.i., Cukrovarnická 10, 162 53, Prague 6, Czech Republic, [‡]Faculty of Mathematics and Physics, Charles University, Ke Karlovu 3, 121 16 Prague 2, Czech Republic, and [∥]IPCMS—DON Unité Mixte, UMR 7504, CNRS—ULP, 23 rue du Loess, BP 43, 67034 Strasbourg Cedex 2, France, and [§]Van der Waals-Zeeman Institute, University of Amsterdam, Valckenierstraat 65, NL-1018 XE Amsterdam, The Netherlands

ABSTRACT Diamond-based materials possess many unique properties, one of them being a broad-band visible photoluminescence due to a variety of color centers. However, a high material refractive index makes the extraction of photoluminescence (PL) from a diamond layer inefficient. In this paper, we show that by periodical nanopatterning of the film's surface into a form of two-dimensional photonic crystal, the extraction of PL can be strongly enhanced within the whole visible spectrum compared to the extraction of PL in a pristine or randomly nanopatterned film. On the basis of theoretical calculations, enhancement is shown to be due to the photonic crystal effect, including efficient coupling of an excitation laser into the diamond.

KEYWORDS: photonic crystals · spontaneous emission · light extraction · diffraction · nanocrystalline diamond films

Diamond-based materials exhibit an unique combination of physical properties, such as extreme hardness, high acoustic velocity, high breakdown field, high thermal conductivity, and many others.[1] Hence diamond as a matrix can support high optical power and high electrical current. Its potential use covers many different fields from electronic devices operating at high frequency, high speed, high power, or extreme conditions through various opto-mechanic, acousto-optics devices, quantum information processing to its use in bio applications due to biocompatibility, and chemical inertness. Diamond has a wide bandgap of 5.5 eV, corresponding to a far UV excitonic luminescence at 225 nm, stable even at high temperatures.[2] By introducing defects and impurities, efficient subgap luminescence can be achieved.[3] Single nitrogen-vacancy (N-V) centers, for example, show a photostable photoluminescence (PL) at room temperature[4] with controllable blinking effects,[5] which makes them especially promising for quantum information processing[6] and single photon generation.[7] The efficient collection of this emission, however, is strongly limited by the large solid angle of the total internal reflection because of the high refractive index of diamond. Therefore, light generated in the thin film is mostly coupled to the guided modes of the structure. In general, light extraction efficiency from such a structure can be increased by introducing scattering centers, or even two-dimensional (2D) photonic crystals (PhC) inside the planar layer. If the PhC penetrates through the whole layer and the part of the emission spectrum lies within the photonic band gap, then the emission into the guided modes is decreased and therefore extracted out of plane. This is called the band gap approach.[8−10] The second approach is based on the idea that a relatively thin PhC structure placed at the top of the active layer and having a lattice constant comparable to the material emission wavelengths can act as a Bragg diffraction grating.[11,12] Simultaneously, the filling factor f (ratio between the material/air surface area) should lie within the interval of $f \approx 0.3-0.6$,[12] and the height of the PhC should be comparable to the remaining layer thickness[13] to obtain the maximal possible extraction efficiency. However, neither of these methods have been so far utilized in order to increase the extraction of the intrinsic light emission from diamond.

In our contribution we apply the latter idea and compare the effect of two different nanopatternings of thin nanocrystalline-diamond (NCD) layers on the extraction efficiency of the PL in the vertical direction (with respect to the thin film plane). The first structure is a NCD layer with shallow 2D-PhC and the second one, used as a reference sample, consists of randomly

*Address correspondence to ondic@fzu.cz.

Received for review August 25, 2010 and accepted December 15, 2010.

Published online December 28, 2010. 10.1021/nn1021555

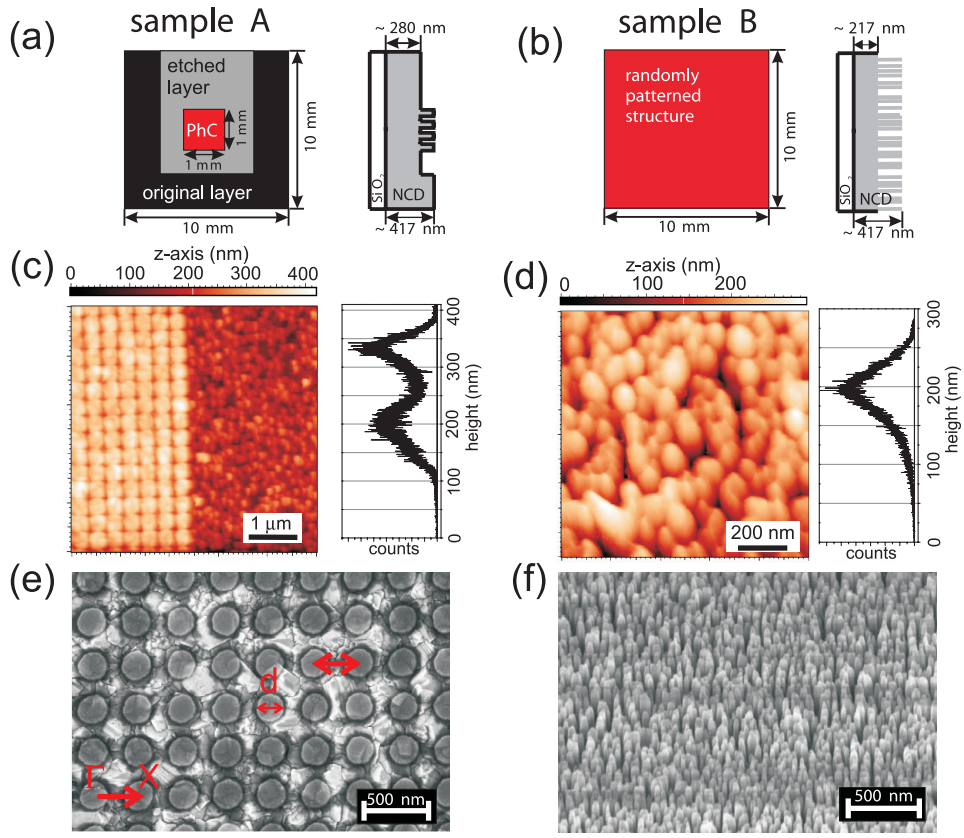

Figure 1. Characteristics of prepared samples. Left column refers to a periodically patterned sample A and right column to a randomly patterned sample B. (a,b) Schematic top-view and cross-section (not in scale) of the sample macroscopic structure. (c,d) AFM scan and height of pillars estimated from the measurement; (e,f) SEM picture.

distributed nanopillars with narrow spacing. We employ two different experimental methods, the first providing us with qualitative and the second providing us with spectrally resolved information about the vertical PL. Both methods reveal strong enhancement of PL extraction from PhC compared to reference samples.

RESULTS AND DISCUSSION

Samples were prepared by nanopatterning of the NCD layers grown on quartz substrate (surface area of 10×10 mm^2). These layers exhibit relatively strong subgap PL in the visible region[14] that could be even increased by employing an additional nitrogen dopping. The thickness of the NCD films, estimated from the position of the Fabry−Pérot peaks in transmission measurements (not shown here), was ~417 nm. First, the shallow 2D-PhC with the surface area of 1×1 mm^2 placed in middle of sample A (Figure 1a) was prepared by electron beam litography. The PhC consists of diamond nanopillars ordered into the square lattice with the following parameters: lattice constant $\Lambda \approx 350$ nm chosen in order to satisfy the Bragg diffraction condition[15] for the whole diamond emission spectrum (400−800 nm); the diameter of nanopillar $d \approx 220$ nm (which leads to $f \approx 0.31$) and the height of 135 ± 15 nm as obtained from the SEM (Figure 1e) and AFM measurements (Figure 1c), respectively. Hence, below the PhC remained the ~280 nm thick nonstructured NCD layer (Figure 1a, cross-section).

As a reference sample, besides the original NCD layer, we used sample B with randomly distributed diamond nanopillars prepared on the entire surface of the layer (Figure 1b). The randomly oriented nanopillars were 30 ± 10 nm in diameter (Figure 1f) and up to 200 nm in height (Figure 1d).

The qualitative comparison of the vertical PL from diverse structures placed side-by-side was investigated using a fluorescence microscope. Bright field images of sample B being placed next to the edge of a nonpatterned layer and sample A with part of the PhC structure area (small rhombuses in the middle are the litography markers) are shown in Figure 2 panels a and c, respectively. First, we compare the PL in the red spectral region (575−625 nm) from both structures under green excitation (530−550 nm). It is obvious that in the case of sample B and the nonpatterned layer, nearly no PL emission is outcoupled into the vertical direction; most of the PL is guided within the layer and can be observed at the sample edges (in the middle of the Figure 2b). The small fraction of the generated light is diffracted on the surface defects or scratches on the surface, evidenced by red spots. On the other hand, compared to the nonpatterned and randomly nanopatterned layers, the PL emission into the vertical direction

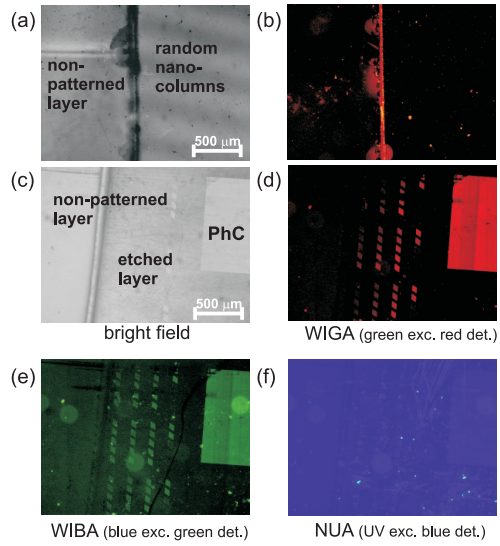

Figure 2. Image from fluorescence microscope. (a) Bright field and (b) WIGA (green excitation and red detection) image of nonpatterned NCD layer compared to randomly nanopatterned layer of sample B. (c) Bright field, (d) WIGA (green excitation and red detection), (e) WIBA (blue excitation and green detection) and (f) NUA (UV excitation and blue detection) image of the PhC structure compared to the surrounding nonpatterned original NCD layer in sample A. Light out-coupling from the PhC is clearly enhanced in the case of the red and green detection.

is greatly enhanced under the same experimental conditions from the PhC structure (Figure 2d). The similar effect of enhanced extraction efficiency on the PhC is obtained with a blue excitation (460−495 nm) and detection in a green spectral region (510−550 nm) (Figure 2e), whereas it does not occur for an UV excitation (360−370 nm) and detection in a blue spectral region (420−460 nm) (Figure 2f), which is probably due to the low intensity of diamond intrinsic PL in the blue spectral region.

Spectrally resolved PL spectra of the PhC structure in sample A, randomly patterned sample B and nonpatterned layer obtained by micro-PL measurements (subgap excitation and detection from the top) are compared in Figure 3. The original nonpatterned PL spectra of the NCD layer are spectrally broad between 400 nm and more than 700 nm with the oscillations due to Fabry−Pérot resonances between the quartz substrate and the diamond−air interface. Sample B PL spectrum agrees with a broad PL of NCD layer and does not show any enhancement. Here, the emitted light with wavelengths much higher than diameters of randomly positioned pillars "feels" only a negligible material perturbation and behaves as it was passing through a quasi-homogeneous layer, and therefore no diffraction and only some scattering can occur. On the other hand, the PL intensity of the PhC in sample B shows strong enhancement in the vertical direction, when compared to the other layers. The ratio of the PL intensity of the PhC in sample A and original unetched NCD layer (Figure 3, gray line) reveals ~6-fold enhancement of PL intensity near 600 nm. We would obtain a very similar ratio of the PL intensity if we consider sample B instead of the original layer.

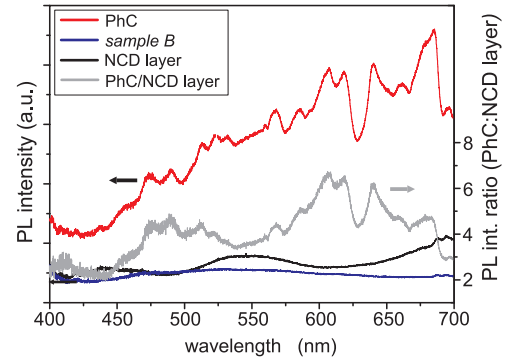

Figure 3. PL emission spectra measured by a micro-Raman Renishaw spectrometer setup (excited by HeCd at 325 nm c.w., 0.3 mW, detected by CCD). The three different types of layers were examined—nonpatterned reference region (black curve), randomly positioned nanopillars (sample B; blue curve), and PhC structure in sample A (red curve). Ratio of the PL intensity of the PhC and original unetched NCD layer is depicted by the gray line showing 6-fold enhancement of light extraction near 600 nm.

Observed enhancement might originate from several effects: (i) the increased number of emitting centers by introducing more surface defects during the sample etching; (ii) influence of adsorbed water;[14] (iii) increased scattering/diffraction of the excitation laser on the nanopatterned surface;[16] (iv) enhanced Fabry−Pérot resonances;[11,17] (v) photonic crystal effect.[11,12] Since effects (i) and (ii) should be of a comparable magnitude in both structures, or even stronger in sample B because of higher surface area, we can conclude that they are not the dominant ones. The scattering/diffraction effect (iii) of the excitation laser will be stronger in the case of the PhC, which in this case works as a 2D diffraction grating with sizes comparable to the excitation wavelength that directly couple light from the pump laser into the layer. This may lead to enhanced pumping efficiency due to the multiple passage of the excitation within the NCD layer, thus increasing the number of emitting centers which finally contribute to the increase of the overall PL intensity. Fabry−Pérot contribution to the outcoupled PL emission (iv) of the PhC originates from the simple fact that the thickness of the PhC and the underlying NCD layer is comparable, but on the other hand their refractive index is different (effective refractive index of the PhC is ~1.6 if we consider the refractive index of diamond to be ~2.4 for the whole visible spectrum). Therefore, in the first approximation, the structure behaves as a bilayer in which the Fabry−Pérot resonances are enhanced compared to the original layer or randomly patterned layer. The PhC effect (v) (present only in the PhC) can be understood from the photonic band structure calculation. The projected band structure of the PhC (Figure 4), including the diamond material underneath, was calculated using a conjugate gradient plane-

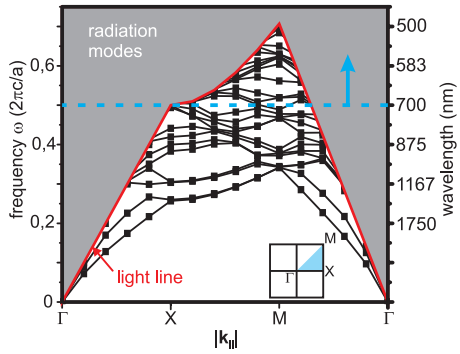

Figure 4. Projected band structure. Computed band structure[18] for the PhC (sample A). Modes lying inside an air light cone (shaded area) are effectively extracted from the layer due to the Bragg diffraction. PL emission spectrum of diamond is above the blue dashed line allowing most of the light to be outcoupled from the layer.

wave expansion method.[18] Modes lying below the air light line (defined as $\omega = c|\mathbf{k}_0|$, where $\mathbf{k}_0$ is the in-plane wave vector in air) are guided modes, localized to the plane of the slab. On the other hand, modes lying in the light cone (shaded area in Figure 4 above the air light line) with the in-plane wave vector of the emitted light propagating inside the layer $|\mathbf{k}| < |\mathbf{k}_0|$ can be diffracted on the PhC and become "leaky" modes that propagate easily to the free space. A phase matching condition $\mathbf{k}_0 = \mathbf{k} \pm \mathbf{G}$ ($\mathbf{G}$ is a reciprocal lattice vector of the PhC) needed in order to obtain Bragg diffraction is fulfilled for these modes due to the continuum of available radiation modes above the light line,[8,9] and therefore they can be efficiently extracted from the layer.

Under our conditions, we continuously excite a number of defect centers, which radiatively emit different colored light that is coupled to the modes of the NCD layer. These modes would be usually guided in a nonpatterned layer; however, due to the presence of the PhC, most of them appear above the light line in the photonic band structure of our sample (Figure 4) and thus can effectively radiate into the free space. On the basis of the parameters of the micro-PL detection, the apex angle of the detection cone was ~60 degrees which covered a large portion of the diffracted light that was propagating to all symmetry directions of the PhC. In terms of the photonic band structure diagram it means our detection covered most of the "leaky" modes lying simultaneously above the air light line and above the blue dashed line, which represents the marginal detected wavelength. The PhC effect and the Fabry–Pérot resonances together explain the fine structure of the PL emission in Figure 3.

CONCLUSION

We have prepared two types of nanopatterned NCD layer: (i) sample A consisting of a nonpatterned NCD layer reference area and a 2D-PhC layer with the square lattice symmetry and (ii) sample B with randomly positioned nanopillars. The PhC structure in sample A showed approximately 6-fold enhancement of the vertical PL intensity near 600 nm when compared to the nonpatterned areas and sample B. By comparison with the random nanopatterning, influence of the scattering centers, the possibly increased number of the surface defects and other surface related effects can be ruled out. Most of the enhancement of light extraction can be thus attributed to the Bragg diffraction of the formerly guided modes on PhC superimposed on the Fabry–Pérot background. In addition, efficient input coupling of the pump laser on the PhC contributes to the enhancement. Further investigations, such as angular far-field PL measurements, are needed to resolve these contributions in more detail. Nevertheless, the observed effect is promising for taking advantage of the diamond PL in optical, opto-electronic, and biological applications. For instance, it could be used to increase external quantum efficiency of the diamond LEDs or improve light coupling into diamond waveguiding structures.

METHODS

Sample Preparation. The NCD films were grown by microwave plasma-assisted chemical vapor deposition (CVD) using an ellipsoidal cavity resonator (Aixtron P6, GmbH). Before the CVD growth, high quality quartz substrates (UQG, Ultrasil, 10 × 10 × 1 mm^3) were cleaned in isopropyl alcohol and dried by a nitrogen gun. Then, they were seeded in a liquid suspension of ultradispersed detonation diamond powder with an average size of *ca.* 5–10 nm in diameter (NanoAmando, New Metals and Chemicals Corp. Ltd., Kyobashi) using an ultrasonic treatment procedure for 40 min (for details, see ref 19). The NCD films were grown in hydrogen (99%) and a methane (1%) based gas mixture. The CVD process parameters were as follows: microwave power 1.4 kW, 1% methane in hydrogen, total gas pressure 30 mbar, and the substrate temperature 560 °C. There was no applied additional nitrogen dopping.

2D-PhC in sample A was fabricated as follows: the NCD films were coated with electron sensitive polymer (PMMA, 120 nm in thickness). The PMMA polymer was nanopatterned by electron beam lithography (EBL) using "*e*-LiNE system" (Raith GmbH) forming the base matrix with regularly repeated openings (250 ± 5 nm in diameter) ordered into a square lattice with a lattice constant of $\Lambda \approx 350$ nm. Then, a nickel layer of 25 nm thickness was evaporated and processed by lift-off strategy to form a masking matrix. Plasma etching by using capacitively coupled RF-plasma in a CF_4/O_2 gas mixture (Phantom LT RIE System, Trion Technology) (for parameters of etching process see ref 20) led to formation of geometrically ordered nanopillars (PhC structure) with the surface area of 1 × 1 mm^2 placed in the middle of the sample A and surrounded by the nonpatterned etched and the original unetched NCD planar area.

Randomly distributed nanopillars in sample B were fabricated as follows: the nanocrystalline diamond films were coated with a 3 nm thin nickel layer using an evaporation process. Then, the samples were treated for 5 min in hydrogen plasma (total gas pressure 30 mbar, microwave power 1300 W, substrate temperature about 600 °C) to form nanosized Ni particles. The diameter of formed nickel nanoparticles ranged from 15 to 25 nm, and these were quasi-homogeneously distributed over the

whole NCD surface. NCD samples covered with Ni nanoparticles, which were used as the masking material, were structured by plasma etching. Details of the fabrication process can be found in ref 20.

Finally, the remaining nickel mask on both types of samples was removed by wet etching in nitro-hydrochloric acid for 5 min.

Characterization. Atomic force microscopy (AFM) images were taken in tapping mode using silicon tip Multi75Al. Scanning electron microscopy (SEM) pictures were obtained with eLINE system Raith GmbH microscope using an accelerating voltage of 10 kV and working distance of 8 mm.

Optical Measurements. All the spectra presented in this study are corrected for the spectral response of the experimental setup. Direct qualitative comparison of the photoluminescence from different samples was obtained with a fluorescence microscope system Olympus IX71 with an objective UPlanFL N 4× (numerical aperture of 0.13). Spectrally resolved vertical PL was measured at room-temperature using the micro-PL spectroscopy system Renishaw (InVia REFLEX) in backscattering geometry. A continuous-wave HeCd laser with an excitation wavelength of 325 nm and power of ~0.3 mW was focused on the sample using a microscope objective lens Leica NPlan 40× (numerical aperture = 0.5, excitation spot diameter, ~3 μm) in the normal direction. The PL emission was collected by the same objective as used for focusing the excitation beam coupled to a charge coupled device (CCD)

Acknowledgment. This work was supported by the Centrum MŠMT (Grant No. LC510), GAAV (Grant No. KJB100100903), GAUK (Grant No. 73910 and Grant No. SVV-2010-261306), AVČR (Grant No. KAN400100701), AVČR (Grant No. M100100902), the Institutional Research Plan (Grant No. AV0Z 10100521), and the Fellowship J. E. Purkyně.

REFERENCES AND NOTES

1. Nebel, C. E. From Gemstone to Semiconductor, *Nat. Mater.* **2003**, *2*, 431–432.
2. Takeuchi, D.; Makino, T.; Kato, H.; Ogura, M.; Tokuda, N.; Oyama, K.; Matsumoto, T.; Hirabayashi, I.; Okushi, H.; Yamasaki, S. Electron Emission from a Diamond (111) p-i-n(+) Junction Diode with Negative Electron Affinity during Room Temperature Operation. *Appl. Phys. Express* **2010**, *3*, 041301.
3. Zaitsev, A. M., *Optical Properties of Diamond: A Data Handbook*; Springer: Berlin, 2001.
4. Gruber, A.; Drabenstedt, A.; Tietz, C.; Fleury, L.; Wrachtrup, J.; von Borczyskowski, C. Scanning Confocal Optical Microscopy and Magnetic Resonance on Single Defect Centers. *Science* **1997**, *276*, 2012–2014.
5. Bradac, C.; Gaebel, T.; Naidoo, N.; Sellars, M. J.; Twamley, J.; Brown, L. J.; Barnard, A. S.; Plakhotnik, T.; Zvyagin, A. V.; Rabeau, J. R. Observation and Control of Blinking Nitrogen-Vacancy Centres in Discrete Nanodiamonds. *Nat. Nanotechnol.* **2010**, *5*, 345–349.
6. Prawer, S.; Greentree, A. D. Applied Physics—Diamond for Quantum Computing. *Science* **2008**, *320*, 1601–1602.
7. Babinec, T. M.; Hausmann, B. J. M.; Khan, M.; Zhang, Y.; Maze, J. R.; Hemmer, P. R.; Lončar, M. A Diamond Nanowire Single-Photon Source. *Nat. Nanotechnol.* **2010**, *5*, 195–199.
8. Fan, S.; Villeneuve, P. R.; Joannopoulos, J. D.; Schubert, E. F. High Extraction Efficiency of Spontaneous Emission from Slabs of Photonic Crystals. *Phys. Rev. Lett.* **1997**, *78*, 3294–3297.
9. Fujita, M.; Takahashi, S.; Tanaka, Y.; Asano, T.; Noda, S. Simultaneous Inhibition and Redistribution of Spontaneous Light Emission in Photonic Crystals. *Science* **2005**, *308*, 1296–1298.
10. Ryu, H. Y.; Lee, Y. H.; Sellin, R. L.; Bimberg, D. Over 30-fold Enhancement of Light Extraction from Free-Standing Photonic Crystal Slabs with InGaAs Quantum Dots at Low Temperature. *Appl. Phys. Lett.* **2001**, *79*, 3573–3575.
11. Wierer, J. J.; David, A.; Megens, M. M., III. Nitride Photonic-Crystal Light-Emitting Diodes with High Extraction Efficiency. *Nat. Photonics* **2009**, *3*, 163–169.
12. Wiesmann, Ch.; Bergenek, K.; Schwarz, U. T. Photonic Crystal LEDs—Designing Light Extraction. *Laser Photonics Rev.* **2009**, *3*, 262–286.
13. David, A.; Benisty, H.; Weisbuch, C. Optimization of Light-Diffracting Photonic-Crystals for High Extraction Efficiency LEDs. *J. Disp. Technol.* **2007**, *3*, 133–148.
14. Dzurnak, B.; Trojanek, F.; Preclikova, J.; Kromka, A.; Rezek, B.; Maly, P. Subgap Photoluminescence Spectroscopy of Nanocrystalline Diamond Films. *Diamond Relat. Mater.* **2009**, *18*, 776–778.
15. Carrol, J.; Whiteaway, J.; Plumb, D. *Distributed Feedback Semiconductor Lasers*; IEE Circuits, Devices and Systems Series; Industrial Electronic Engineers: London, 1998; Vol. 10.
16. Erchak, A. A.; Ripin, D. J.; Fan, S.; Rakich, P.; Joannopoulos, J. D.; Ippen, E. P.; Petrich, G. S.; Kolodziejski, L. A. Enhanced Coupling to Vertical Radiation Using a Two-Dimensional Photonic Crystal in a Semiconductor Light-Emitting Diode. *Appl. Phys. Lett.* **2001**, *78*, 563–565.
17. Bergenek, K.; Wiesmann, Ch.; Wirth, R.; O'Faolain, L.; Lindner, N.; Streubel, K.; Krauss, T. F. Enhanced Light Extraction Efficiency from AlGaInP Thin-Film Light-emitting Diodes with Photonic Crystals. *Appl. Phys. Lett.* **2008**, *93*, 041105.
18. Johnson, S. G.; Joannopoulos, J. D. Block-Iterative Frequency-Domain Methods for Maxwell's Equations in a Planewave Basis. *Opt. Express* **2001**, *8*, 173–190.
19. Kromka, A.; Rezek, B.; Remes, Z.; Michalka, M.; Ledinsky, M.; Zemek, J.; Potmesil, J.; Vanecek, M. Formation of Continuous Nanocrystalline Diamond Layers on Glass and Silicon at Low Temperatures. *Chem. Vap. Deposition* **2008**, *14*, 181–186.
20. Babchenko, O.; Kromka, A.; Hruska, K.; Kalbacova, M.; Broz, A.; Vanecek, M. Fabrication of Nanostructured Diamond Films for SAOS-2 Cell Cultivation. *Phys. Status Solidi A* **2009**, *206*, 2033–2037.